A Quest for New Antimalarial Agents with Improved Specificity Guided by Molecular Docking, 3D QSAR and Molecular Dynamics Simulation Studies

Janaiah Chevula, Saikrishna Balabadra, Sree Kanth Sivan and Vijjulatha Manga[*]

Molecular Modeling and Medicinal Chemistry Group, Department of Chemistry, University College of Science, Osmania University, Hyderabad-500 007, India

*Corresponding author: Fax: +91 40 27090020; Tel: +91 40 27682337; E-mail: vijjulathamanga@gmail.com

Chloroquine (CQ)-resistance strain of *Plasmodium falciparum* is posting as an alarming hitch in curing malarial disease. Efforts are on to overcome this drug resistance and to produce potential inhibitors. In this context, three-dimensional quantitative structure-activity relationship (3D-QSAR) and docking studies were extended out for recently reported 4-aminoquinoline rhodanine, 4-aminoquinoline tetrazoles, 4-anilinoquinoline triazines, 9-anilinoacridine triazines. The model generated showed good correlation coefficients r^2 (0.961 and 0.965) and test set prediction coefficients r^2 (0.600 and 0.620); all reinforce showed the good predictive competence of the QSAR model derived. Based on outcome of results we designed new inhibitors. These newly designed molecules were docked into active site of protein. The docking results revealed that these molecules not only interact specifically with Glu 122 in the NADH binding pocket as that of best active compound but also showed additional interactions with Leu 115. Further, molecular dynamics simulations were also carried which reinforced the docking results and showed that the newly designed molecules formed more stable complexes when compared to existing ligands. Furthermore these molecules retained interactions with active site amino acid residue Glu 122 for more percentage of simulation time which is crucial for enhancing inhibitory activity. Therefore it can be concluded that these newly designed molecules can further be modified so as to generate more potent anti malarial lead structures in near future.

Keywords: 4-Aminoquinoline hybrids, pf3D7 Strain, Molecular docking, 3D-QSAR, Molecular dynamics simulation.

INTRODUCTION

Malaria continues to be one of the major causes of morbidity even today since its discovery. It is mainly caused by *Plasmodium falciparum* and is prevalent in sub-tropical countries. Due to vituperative nature it drastically affected the health of the people and created a financial setback in developing countries. To ease this problem United Nation Development Program (UNDP) has mentioned this as a millennium development goal. The inefficient control of this disease is due to lack of novel anti plasmodial drugs [1], transpiring resistance [2] and slow progress in the development of new approved vaccines [3]. Further resistance of Plasmodium species towards primaquine, artemisinin and quinoline based drugs have contributed to its wide spread. Hence, there is an urgent need to develop new drugs which can help in combating malaria.

Mutations in the active sites of receptors are primarily responsible for drug resistance. Lactate dehydrogenase (LDH)

enzyme of *P. falciparum* is considered to be a prospective target to fight drug resistance and increased specificity in human malaria. Lactate dehydrogenase enzyme is essential for the production of energy, it catalyzes the formation of lactate in the ultimate stage of glycolysis pathway by converting pyruvate. *Plasmodium falciparum* lactate dehydrogenase (pfLDH) has been chosen for the present study due to its distint active site and substrate specificity. The emergence of resistance towards commonly employed drugs like chloroquine, quinine, and mefloquine has limited 4-amino-quinoline scaffold in treatment of malaria [4]. Hence, it has essential compulsory to investigate efficacious drugs which can efficiently tackle malaria. Therefore, in present study we employed integrated molecular docking, 3D-QSAR and molecular dynamics (MD) simulation approaches on 4-aminoquinoline derivatives in order to explore the probable binding modes and derive key structural features to enhance their inhibitory activity.

EXPERIMENTAL

A total of 70 molecules [5-8] with known inhibition of pf 3d7 strain were taken for the present study. Linux operating system was used for molecular modeling calculations. The crystal structure of pf LDH bound with chloroquine inhibitor (pdb id: 1CET) [9] was downloaded from RCSB protein data bank. Docking studies were performed using GLIDE 5.6 using Extra precision (XP) docking mode [10] active site of the receptor was made flexible by scaling the van der Waals region to 0.9 [11], this approach softens active site region [12]. The low energy conformers of the ligands were obtained by applying OPLS 2005 force field. Structures of the molecules are given in Table-1, their IC_{50}, pIC_{50} and dock score values are given in Table-2. Most promising poses of ligands obtained from docking were subjected to 3D QSAR analysis [13,14]. CoMFA and CoMSIA studies were carried out as reported earlier [15-17] using SYBYLX -2.1 [18] by applying Gasteiger-Huckel [19] charges. CoMFA and CoMSIA models were developed using training set of 50 molecules by applying PLS analysis. Predictive ability of the models was determined using test set of 20 molecules.
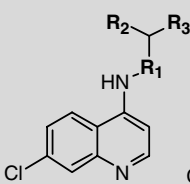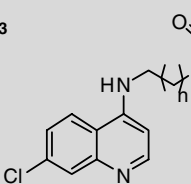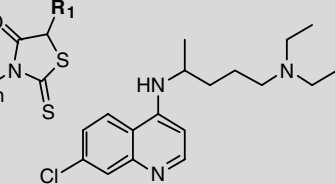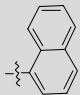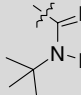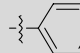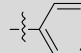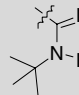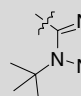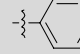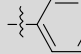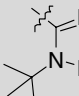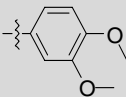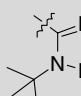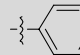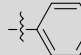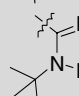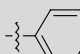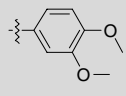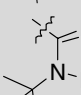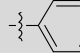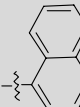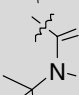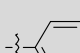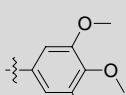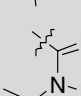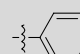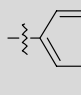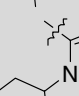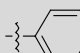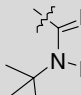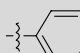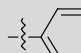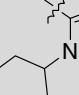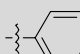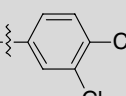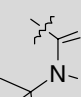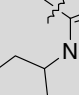
Molecular dynamics simulation: Desmond 3.8 [20] was used for molecular dynamics simulations, in order to investigate and compare the binding modes of chloroquine, molecule 49 and newly designed molecule N1. Molecular dynamics simulations were carried out as per the procedure [21] and the root mean square deviations (RMSD) were examined during course of simulation and interaction diagrams of the simulation were also generated to check the stability of hydrogen bond interactions.

RESULTS AND DISCUSSION

Plasmodium falciparum CQ-sensitive inhibitors were docked into the active site (Val 26, Phe 52, Asp 53, Ile 54, Val 55, Tyr 85, Ala 98, Gly 99, Phe 100, Lys 118, Ile 119 and Glu122) of pfLDH. Dock pose of most active molecule 49 is depicted in Fig. 1.

3D QSAR analysis was performed using a set of 70 molecules which were divided into training and test set of 50 and 20, respectively. The statistical results of CoMFA and CoMSIA are summarized in Table-3. The statistical analysis yielded q^2_{loo} of 0.547

TABLE-1
DATABASE OF MOLECULES

| S. No | R₁ | R₂ | R₃ | S. No | R₁ | R₂ | R₃ |

S. No.	n	R₁	S. No.	n	R₁	S. No.	n	R₁
14	1	H	21	3	styryl-4-NO₂	28	2	styryl-4-Cl
15	2	H	22	3	styryl-4-N(CH₃)₂	29	2	styryl-4-N(CH₃)₂
16	3	H	23	2	styryl-3,4,5-trimethoxy	30	2	styryl-2-NO₂
17	3	styryl	24	2	styryl-naphthyl-OCH₃	31	1	styryl
18	3	styryl-4-ethyl	25	2	styryl-4-NO₂	32	1	styryl-4-ethyl
19	3	styryl-4-pyridyl	26	2	styryl-3-NO₂	33	1	styryl-3,4,5-trimethoxy
20	3	styryl-2-furyl	27	2	styryl-4-F			

(34-42)   (43-64)   (65-69)

S. No.	R₁	R₂	S. No.	R₁	R₂
34	–NH–phenyl	–N(piperazine)N–CH₃	52	–NH–phenyl	–NH₂
35	–NH–phenyl	–NH–CH₂CH₂–N(morpholine)O	53	–NH–phenyl	–N(CH₃)H
36	–NH–phenyl	–NH–CH₂CH₂CH₂–N(morpholine)O	54	–NH–(2-methylphenyl)	–N(piperazine)N–CH₃
37	–NH–phenyl	–NH–CH₂CH₂–N(CH₃)₂	55	–NH–(2-methylphenyl)	–NH–CH₂CH₂–N(C₂H₅)₂
38	–NH–phenyl	–NH–CH₂CH₂CH₂–N(CH₃)₂	56	–NH–(2-methylphenyl)	–NH–CH₂CH₂CH₂–N(morpholine)O
39	–NH–phenyl	–NH–CH₂CH₂–OH	57	–NH–(2-methylphenyl)	–NH–cyclohexyl
40	–NH–phenyl	–NH–NH₂	58	–NH–(2-methylphenyl)	–NH₂

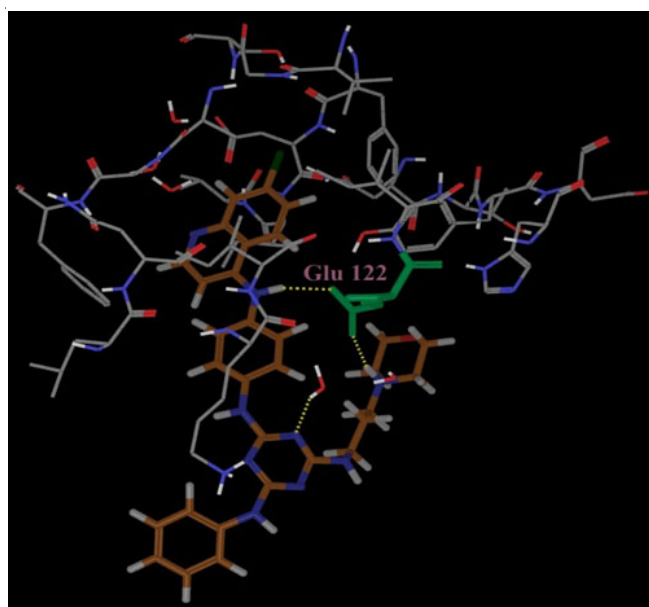|					
41	(chemical structure)	(chemical structure)	59	(chemical structure)	(chemical structure)
42	(chemical structure)	(chemical structure)	60	(chemical structure)	(chemical structure)
43	(chemical structure)	(chemical structure)	61	(chemical structure)	(chemical structure)
44	(chemical structure)	(chemical structure)	62	(chemical structure)	(chemical structure)
45	(chemical structure)	(chemical structure)	63	(chemical structure)	(chemical structure)
46	(chemical structure)	(chemical structure)	64	(chemical structure)	(chemical structure)
47	(chemical structure)	(chemical structure)	65	(chemical structure)	(chemical structure)
48	(chemical structure)	(chemical structure)	66	(chemical structure)	(chemical structure)
49	(chemical structure)	(chemical structure)	67	(chemical structure)	(chemical structure)
50	(chemical structure)	(chemical structure)	68	(chemical structure)	(chemical structure)
51	(chemical structure)	(chemical structure)	69	(chemical structure)	(chemical structure)

Fig. 1. Dock pose of most active molecule 49 showing H-bond interaction with Glu 122 of pfLDH

and 0.533, r^2_{ncv} of 0.961 and 0.965, r^2_{pred} of 0.600 and 0.620, respectively for CoMFA and CoMSIA. The results indicate good internal and external predictive ability of the models. The scatter plots of both CoMFA and CoMSIA are shown in Fig. 2.

Contour analysis: The CoMFA and CoMSIA contour maps were graphically interpreted by field contribution maps using 'STDEV COEFF' field type which represented default 80 and 20 % level contribution for favored and disfavored regions.

Figs. 3a-b show contour maps of steric and electrostatic fields of both CoMFA and CoMSIA, where green and yellow contours represent favored and disfavored regions, respectively. In most active molecule 49, large green contour is seen below phenyl ring attached to triazene, suggesting substitution with bulky group at this position will increase the activity. A yellow contour near the phenyl ring attached to chloroqine suggests bulky substituents in this area will significantly decrease the biological activity. Red contour on triazene ring recommend substitution with electronegative group at this position will increase the activity. Blue contour present on phenyl ring attached

TABLE-2
MOLECULES ALONG WITH THEIR IC$_{50}$, pIC$_{50}$, DOCK SCORE AND PREDICTED ACTIVITIES

| S. No.	IC$_{50}$	pIC$_{50}$	Dock score	Pred CoMFA	Pred CoMSIA	S. No.	IC$_{50}$	pIC$_{50}$	Dock score	Pred CoMFA	Pred CoMSIA
1	120.4	6.919	-5.583	6.926	6.907	*36	15.08	7.822	-4.699	8.129	7.94
2	81.4	7.089	-6.096	7.067	7.094	37	7.95	8.1	-5.572	8.1	8.11
3	57.88	7.237	-5.877	7.181	7.316	38	4.21	8.376	-4.403	8.502	8.573
4	70.58	7.151	-5.019	7.256	7.185	39	9.46	8.024	-6.097	8.054	8.099
5	54.22	7.266	-4.854	7.291	7.261	40	4.27	8.37	-4.953	8.39	8.336
6	10.66	7.972	-5.071	7.725	7.795	41	27.88	7.555	-4.862	7.603	7.579
7	11.01	7.958	-5.176	7.836	7.853	42	20.15	7.696	-4.731	7.654	7.776
8	29.52	7.53	-4.933	7.803	7.798	43	29.74	7.527	-4.550	7.476	7.509
*9	11.78	7.929	-4.960	7.531	7.579	44	38.77	7.412	-4.958	7.404	7.407
10	51.35	7.289	-4.867	7.356	7.373	45	23.13	7.636	-5.328	7.656	7.514
*11	28	7.553	-4.902	7.484	7.502	46	234.63	6.63	-4.619	6.587	6.696
*12	853.4	6.069	-3.920	6.782	6.976	47	5.92	8.228	-4.754	8.229	8.25
*13	92.66	7.033	-1.901	7.48	7.325	48	18.53	7.732	-4.135	7.683	7.73
*14	181	6.742	-5.171	7.043	6.987	49	3.01	8.521	-5.827	8.497	8.496
15	200.1	6.699	-5.410	6.883	6.865	*50	64.84	7.188	-3.306	7.062	6.929
*16	241.6	6.617	-5.469	7.202	7.197	*51	33.65	7.473	-4.525	7.7	7.588
17	43.5	7.362	-4.620	7.365	7.39	52	41.5	7.382	-5.100	7.465	7.385
18	54.5	7.264	-4.468	7.26	7.253	53	19.03	7.721	-5.487	7.725	7.704
*19	93.5	7.029	-4.872	7.446	7.369	54	18.85	7.725	-4.916	7.672	7.692
*20	35	7.456	-5.345	7.176	7.182	55	26.05	7.584	-3.062	7.548	7.538
21	40	7.398	-3.710	7.386	7.379	56	13.42	7.872	-5.493	7.992	7.907
22	31	7.509	-3.221	7.479	7.517	57	162.99	6.788	-1.681	6.739	6.798
23	56	7.252	-5.219	7.201	7.164	58	29.65	7.528	-5.138	7.484	7.426
*24	90.7	7.042	-4.908	7.436	7.362	59	37.63	7.424	-5.298	7.403	7.405
25	23.5	7.629	-4.880	7.633	7.6	60	12.44	7.905	-2.719	7.802	7.89
*26	96	7.018	-4.013	7.4	7.375	61	11.9	7.924	-4.544	7.836	7.876
*27	93.9	7.027	-6.268	7.273	7.22	62	7.03	8.153	-5.215	8.259	8.169
28	76.5	7.116	-5.337	7.178	7.203	*63	11.88	7.925	-4.266	7.58	7.659
*29	49.3	7.307	-4.953	7.413	7.126	*64	6.41	8.193	-4.954	7.707	7.738
30	38.2	7.418	-4.721	7.529	7.325	65	26.3	7.58	-3.451	7.622	7.597
31	58.7	7.231	-4.943	7.139	7.052	66	291.73	6.535	-5.220	6.642	6.652
32	42.7	7.37	-3.873	7.303	7.376	67	110.67	6.956	-5.559	6.985	6.911
33	34.8	7.458	-4.497	7.46	7.449	*68	40.95	7.388	-4.779	7.512	7.68
*34	22.1	7.656	-3.556	7.655	7.733	69	34.56	7.461	-5.849	7.418	7.445
*35	6.97	8.157	-4.679	8.389	8.242	Chloroquine	8.15	8.089	-4.554	7.866	7.923

*Represents test set molecules
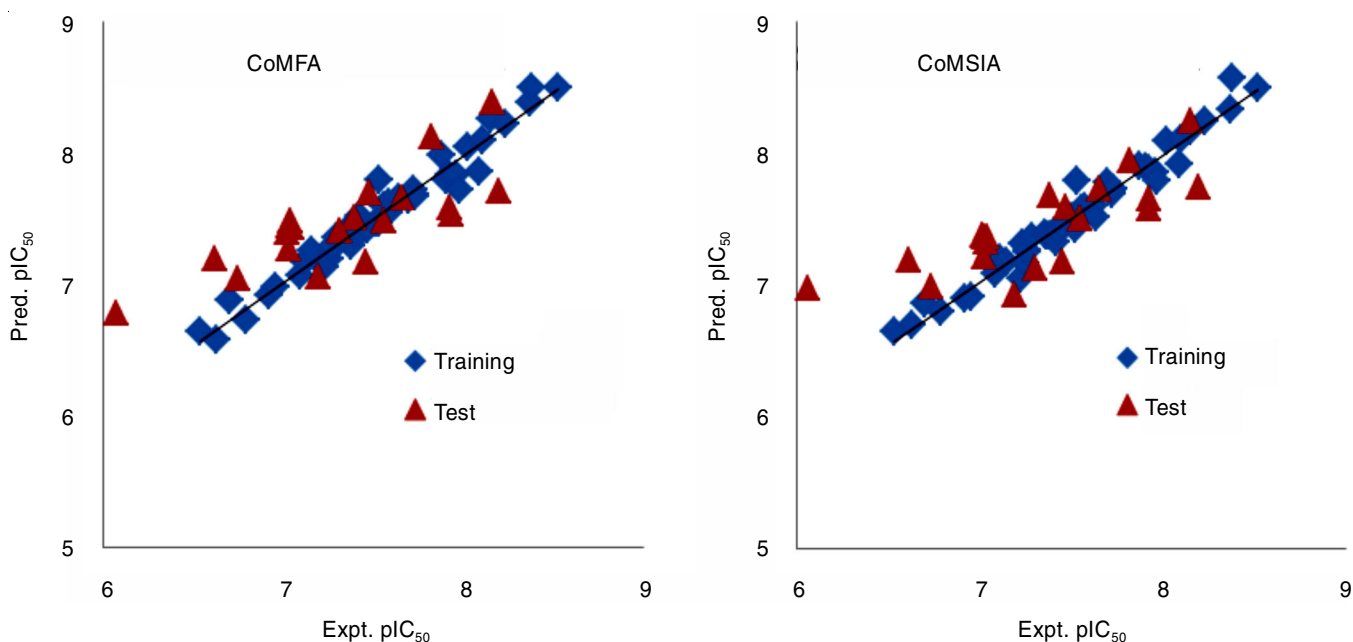
Fig. 2. Scatter plots of predicted *vs* experimental pIC$_{50}$ values (test set is represented as triangles)

TABLE-3
STATISTICAL RESULTS FOR CoMFA AND CoMSIA MODELS

Statistical parameters	CoMFA model	CoMSIA model
q^2	0.547	0.533
Molecules in training set	50	50
Molecules in test set	20	20
ONC	6	5
r^2_{ncv}	0.961	0.965
SEE	0.095	0.089
F	175.629	241.631
r^2_{pred}	0.600	0.620
Fraction of field contributions:		
Steric	0.723	0.157
Electrostatic	0.277	0.167
Hydrophobic	–	0.209
Donor	–	0.237
Acceptor	–	0.230

q^2_{loo} = cross-validated correlation coefficient by leave one out method, r^2_{ncv} = non cross-validated correlation coefficient, ONC = optimum number of components, SEE = standard error of estimate, F = Fisher test value, r^2_{pred} = cross-validated correlation coefficient on test set.

to chloroquine signify that substitution with more electronegative groups at this position will decrease the activity.

Hydrophobic fields are depicted in Fig. 3c, where yellow and white highlighted regions represent hydrophobic and hydrophilic preferred regions, respectively. A large white contour seen close to benzene ring in the most active molecule 49 indicates that substituting bulkier hydrophilic groups will increase the activity. Hydrogen bond donor and acceptor contours in Fig. 3c show cyan and purple, magenta and red for favoured and disfavoured, respectively. For molecule 49 a donor disfavoured purple contour is observed near to NH of quinoline and an acceptor disfavored red contour is observed near to NH of benzene region indicating the decrease in activity.

Designed molecules: The information obtained from the 3D QSAR analysis is illustrated pictorially in Fig. 4, here the molecular area is divided into four regions. Region A is electronegative and hydrophilic favoured, when benzene was substituted with pyranone showed increase in predictive activity.
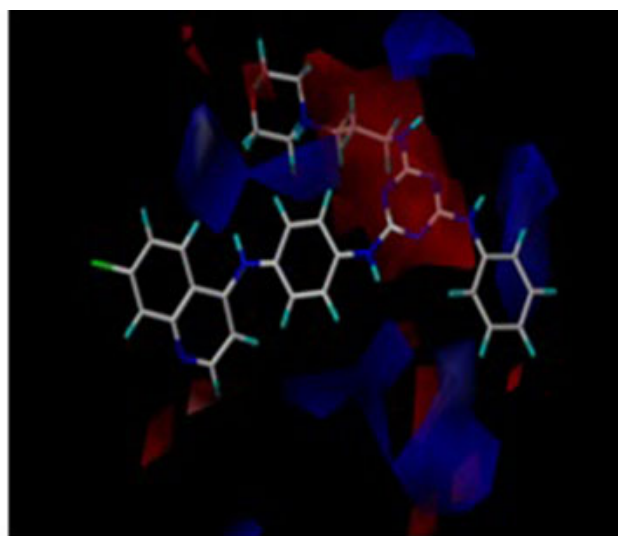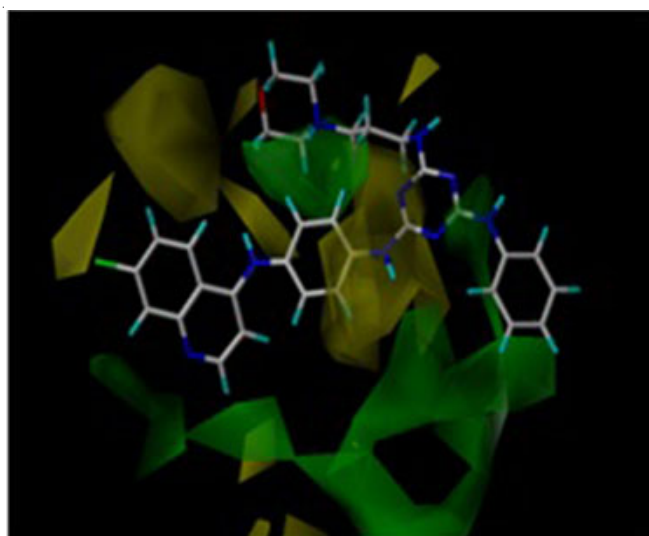

Fig. 3a. CoMFA steric (green is favored and yellow is disfavored), electrostatic (red is more negative charge and blue is more positive charge favored regions) fields contour maps for best active molecule 49
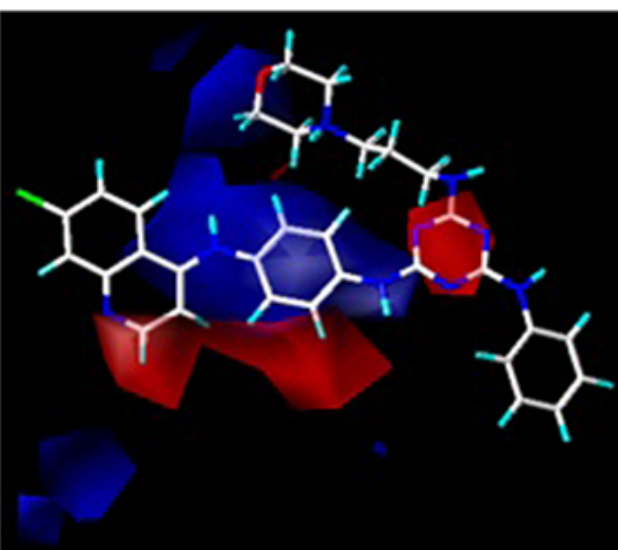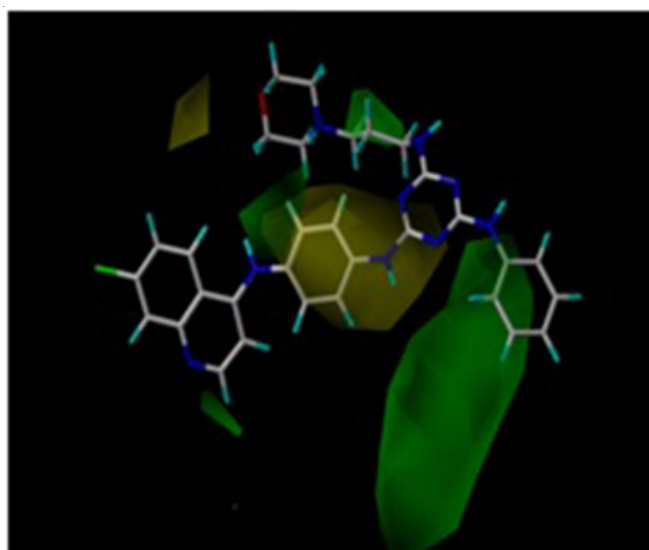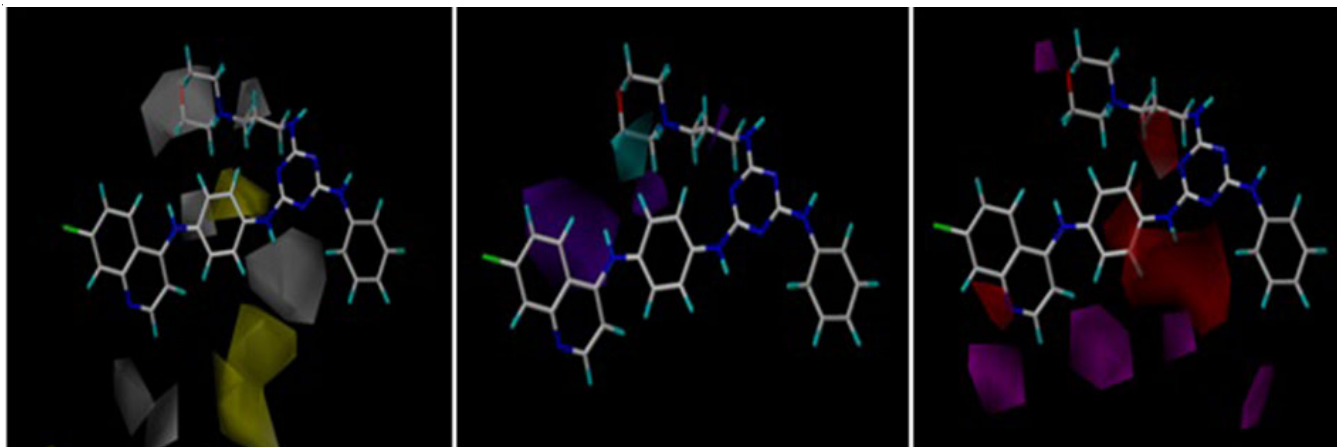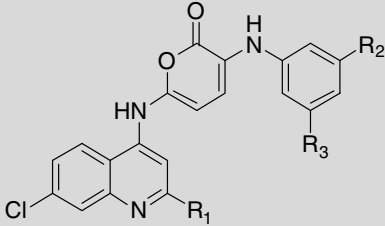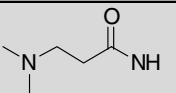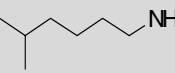

Fig. 3b. CoMSIA Steric (Green is favored and yellow is disfavored), electrostatic (red is more negative charge and blue is more positive charge favored regions) fields contour maps for best active molecule 49
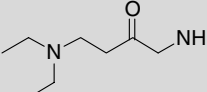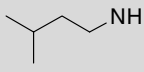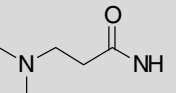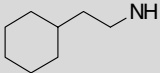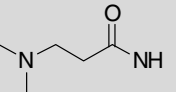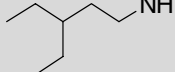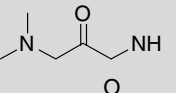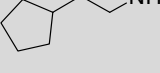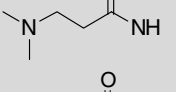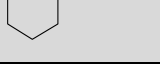
Fig. 3c. CoMSIA contour maps for best active molecule 49, Hydrophobic (white is hydrophilic and yellow is hydrophobic favored region), hydrogen bond donor (cyan is favored and purple is disfavored region), hydrogen bond acceptor (magenta and red are favored and disfavored regions respectively) fields

Region B with steric and hydrophilic favoured, substituents such as -CONH$_2$ has increased the affinity. At region C steric favoured contour maps were observed, hence phenyl ring was substituted with saturated hydrocarbon chains and cyclohexyl rings to improve the activity. At region D, electrostatic favoured contour was observed, hence triazine ring was substituted with simple benzene. These entire contours were taken into consideration to substitute with desirable substituents to obtain tailored Table-4

TABLE-4
DESIGNED MOLECULES ALONG WITH DOCK SCORE AND PREDICTED ACTIVITIES

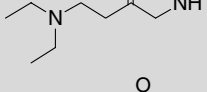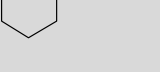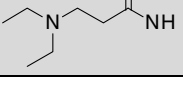| S. No.	R$_1$	R$_2$	R$_3$	Dock score	Pred CoMFA	Pred CoMSIA
N1	Me			-6.183	7.989	8.147
N2	Me			-5.637	8.244	8.120
N3	Me			-5.509	8.137	8.030
N4	H			-5.045	8.168	8.368
N5	H			-5.965	8.220	8.156
N6	H			-4.827	7.903	8.278
N7	H			-5.130	8.212	7.892
N8	Et			-5.751	8.206	8.069
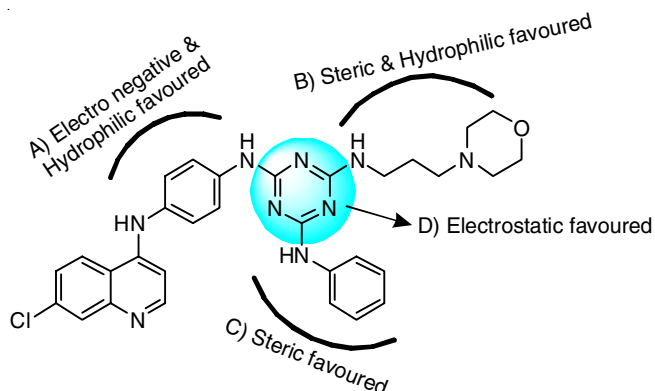
Fig. 4.   Overall analysis of the contours depicting the favorable regions for substitution

Fig. 6.   RMSD of protein back bone as function of simulation time of each complex with respect to initial structure. N1 represents newly designed molecule, CQ represents Chloroquine while 49 represents best active molecule

molecules having high predicted activity towards *Plasmodium falciparum* 3D7 activity.

The designed molecules resembled best active compound in terms of interactions and showed comparable dock score with good predicted activity. Fig. 5 shows dock pose of newly designed molecule N1 that showed two H-bond interactions with Glu 122 and one hydrogen bond with Leu 115 in protein active site of 1CET, hence increased the binding affinity. Predicted pIC_{50} values were calculated and found to be better; structures of newly designed molecules and their predicted pIC_{50} values are given in Table-4.
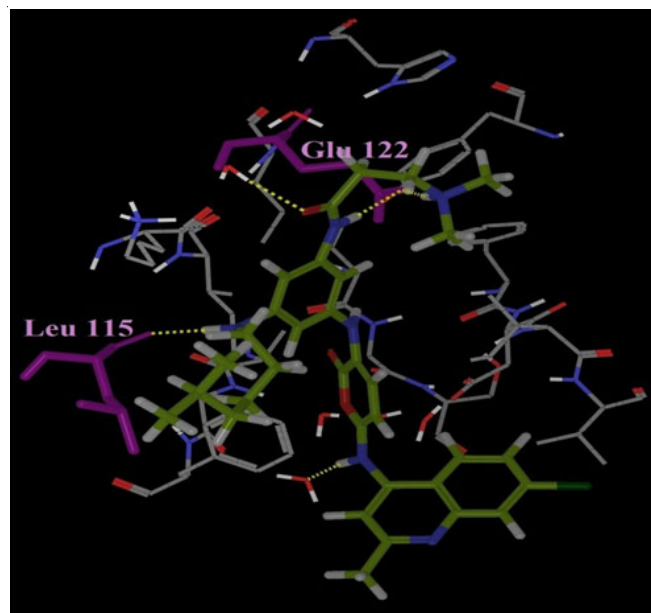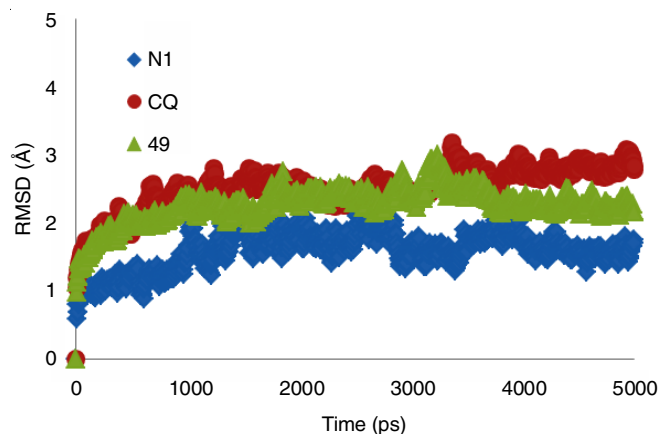

Fig. 5.   Dock pose of designed molecule N1 showing two H-bond interactions with Glu 122 and one hydrogen bond with Leu 115 in the protein active site of 1CET

Molecular dynamics simulations: Molecular dynamics simulation was performed for 5ns on protein ligand complex of chloroquine, molecule 49 and new molecule N1. Fig. 6 shows the RMSD of protein back bone as function of simulation time of each complex with respect to initial structure. The RMSD for chloroquine ranged from 1.056 to 2.826 Å with a maximum RMSD of 3.182 Å during the 5ns simulation time. RMSD for molecule 49 from the series of ligands used in 3D-QSAR studies showed RMSD of 0.984 to 2.169 Å with a maximum RMSD of

3.182 Å during the simulation time indicating its stability which correlates to its better activity than chloroquine. Structural requirement based on 3D QSAR analysis was utilized for designing new molecules and to confirm the stability of these newly designed molecules; molecular dynamics simulations were performed for protein molecule N1 complex. The RMSD for N1 ranged from 0.595 Å to 1.784 Å with a maximum RMSD of 2.384 Å during the 5ns simulation time. The values clearly indicate that N1-Protein complex has better stability. Analysis of protein ligand interactions between pfLDH and ligands was performed to understand mode of binding and changes occurring in binding during simulations.

Glu 122 and Asp 53 are the vital residues for ligand binding. Fig. 7(a-c) shows protein ligand contact interaction over trajectory. The y-axis is normalized over the course of the trajectory. The chloroquine showed major hydrogen bond interaction with Asp 53 and hydrophobic interaction with Ile 54, Phe 100, and Ile 119. In case of molecule 49, it showed hydrogen bond interaction with Asp 53, but during the course of simulation it existed as water mediated bridged hydrogen bond. It retained all the hydrophobic interaction shown by chloroquine and showed more interaction with Val 26, Phe 52, Ala98, and Ile 123. The simulation interaction analysis of designed molecule N1 showed similar interaction with active site residues, direct hydrogen bond interaction was retained with Glu 122 for maximum duration of the simulation time and retained all other hydrophobic interaction as chloroquine. This suggests that the designed molecule N1 has ability to specifically bind to the conserved Glu 122 residue of pfLDH were as in all mammalian and other forms of LDH there is phenylalanine residue at this position that is not capable of forming hydrogen bonding [22].

Conclusion

To pursue novel antimalarials with improved specificity a model was developed using the *in vitro* antimalarial data reported, in order to design molecules with improved activity. QSAR model was statistically significant and the significance was validated. The study has provided insights to improve biological activity with the change in particular rings (anilino phenyl and triazine) in 4-aminoquinoline derivatives. Molecular docking and dynamic simulations studies highlight the exclusive binding
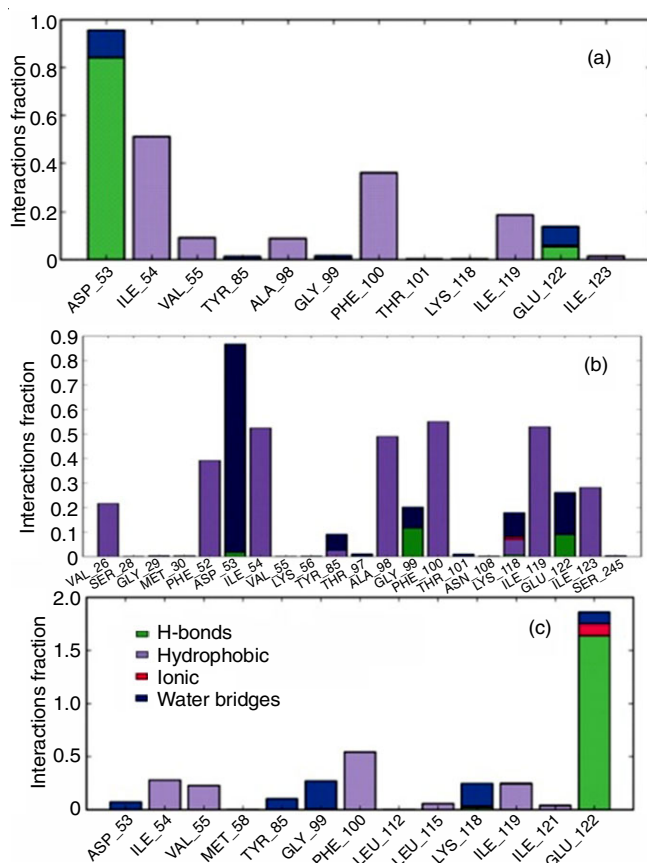
Fig. 7.   Protein – ligand contact interaction over trajectory with respect (a) chloroquine, (b) molecule 49, and (c) molecule N1

signature of the ligands with the active site residue *i.e.* Glu122 of the target and it explains the specificity and subtle differences in their predicted IC_{50} values.

ACKNOWLEDGEMENTS

CONFLICT OF INTEREST

The authors declare that there is no conflict of interests regarding the publication of this article.

REFERENCES

1. E.H. Ekland and D.A. Fidock, *Int. J. Parasitol.*, **38**, 743 (2008); https://doi.org/10.1016/j.ijpara.2008.03.004.
2. D.A. Fidock, *Nature*, **465**, 297 (2010); https://doi.org/10.1038/465297a.
3. M. Wisniewski and D.J. Zak, *Wiad Parazytol.*, **56**, 133 (2010).
4. R.G. Ridley, *Nature*, **415**, 686 (2002); https://doi.org/10.1038/415686a.
5. K. Chauhan, M. Sharma, J. Saxena, S.V. Singh, P. Trivedi, K. Srivastava, S.K. Puri, J.K. Saxena, V. Chaturvedi and P.M.S. Chauhan, *Eur. J. Med. Chem.*, **62**, 693 (2013); https://doi.org/10.1016/j.ejmech.2013.01.017.
6. S. Pandey, P. Agarwal, K. Srivastava, S. RajaKumar, S.K. Puri, P. Verma, J.K. Saxena, A. Sharma, J. Lal and P.M.S. Chauhan, *Eur. J. Med. Chem.*, **66**, 69 (2013); https://doi.org/10.1016/j.ejmech.2013.05.023.
7. A. Kumar, K. Srivastava, S. Raja Kumar, S.K. Puri and P.M.S. Chauhan, *Bioorg. Med. Chem. Lett.*, **19**, 6996 (2009); https://doi.org/10.1016/j.bmcl.2009.10.010.
8. A. Kumar, K. Srivastava, S. Raja Kumar, M.I. Siddiqi, S.K. Puri, J.K. Sexana and P.M.S. Chauhan, *Eur. J. Med. Chem.*, **46**, 676 (2011); https://doi.org/10.1016/j.ejmech.2010.12.003.
9. J.A. Read, K.W. Wilkinson, R. Tranter, R.B. Sessions and R.L. Brady, *J. Biol. Chem.*, **274**, 10213 (1999); https://doi.org/10.1074/jbc.274.15.10213.
10. Schrödinger, LLC, New York, Glide Version 5.6, (2010).
11. R.A. Friesner, J.L. Banks, R.B. Murphy, T.A. Halgren, J.J. Klicic, D.T. Mainz, M.P. Repasky, E.H. Knoll, M. Shelley, J.K. Perry, D.E. Shaw, P. Francis and P.S. Shenkin, *J. Med. Chem.*, **47**, 1739 (2004); https://doi.org/10.1021/jm0306430.
12. D.M. Taverna and R.A. Goldstein, *Proteins*, **46**, 105 (2002); https://doi.org/10.1002/prot.10016.
13. A.P. Zambre, A.L. Ganure, D.B. Shinde and V.M. Kulkarni, *J. Chem. Inf. Model.*, **47**, 635 (2007); https://doi.org/10.1021/ci6004367.
14. S.M. Vadlamudi and V.M. Kulkarni, *Int. Electron. J. Mol. Des.*, **3**, 586 (2004).
15. R.D. Cramer, D.E. Patterson and J.D. Bunce, *J. Am. Chem. Soc.*, **110**, 5959 (1988); https://doi.org/10.1021/ja00226a005.
16. R.D. Cramer III, J.D. Bunce, D.E. Patterson and I.E. Frank, *Quant. Struct. Activ. Relat.*, **7**, 18 (1988); https://doi.org/10.1002/qsar.19880070105.
17. G. Klebe, U. Abraham and T. Mietzner, *J. Med. Chem.*, **37**, 4130 (1994); https://doi.org/10.1021/jm00050a010.
18. Sybyl-X1, 2. Tripos Associates, St. Louis (MO), www.tripos.com/sybyl, (2010).
19. J. Gasteiger and M. Marsili, *Tetrahedron*, **36**, 3219 (1980); https://doi.org/10.1016/0040-4020(80)80168-2.
20. D.E. Shaw, DESMOND (Version 3.8), New York (2014).
21. S.R. Peddi, S.K. Sivan and V. Manga, *J. Rec. Sig. Tran.*, **36**, 488 (2016); https://doi.org/10.3109/10799893.2015.1130057.
22. J. Penna-Coutinho, W.A. Cortopassi, A.A. Oliveira, T.C. Franca and A.U. Krettli, *PLoS One*, **6**, e21237 (2011); https://doi.org/10.1371/journal.pone.0021237.